

Chapter 3

Theoretical Treatment of Helicon Waves

3.1 Dispersion Relation in a Uniform Cold Plasma

The dispersion relation is found by solving the wave equation, with the assumption that first-order quantities vary as $e^{i(\mathbf{k}\cdot\mathbf{r}-\omega t)}$ [106, 71, 81].

$$\mathbf{n} \times (\mathbf{n} \times \mathbf{E}) + \mathbf{K} \cdot \mathbf{E} = \mathbf{0} \quad (3.1)$$

where \mathbf{n} is defined as

$$\mathbf{n} = \frac{c}{\omega} \mathbf{k} \quad (3.2)$$

and the dielectric tensor is

$$K = \begin{pmatrix} S & -iD & 0 \\ iD & S & 0 \\ 0 & 0 & P \end{pmatrix} \quad (3.3)$$

$$S = \frac{1}{2}(R + L) \quad (3.4)$$

$$D = \frac{1}{2}(R - L) \quad (3.5)$$

For a two component plasma with ions and electrons

$$R = 1 - \frac{\omega_{pi}^2}{\omega^2 + \omega\omega_{ci}} - \frac{\omega_{pe}^2}{\omega^2 - \omega\omega_{ce}} \quad (3.6)$$

$$L = 1 - \frac{\omega_{pi}^2}{\omega^2 - \omega\omega_{ci}} - \frac{\omega_{pe}^2}{\omega^2 + \omega\omega_{ce}} \quad (3.7)$$

$$P = 1 - \frac{\omega_{pi}^2}{\omega^2} - \frac{\omega_{pe}^2}{\omega^2} \quad (3.8)$$

where the plasma frequency and cyclotron frequency for ions and electrons are given by

$$\omega_{pi,pe}^2 = \frac{n_e q_{i,e}^2}{m_{i,e} \epsilon_0} \quad (3.9)$$

$$\omega_{ci,ce} = \frac{q_{i,e} B_0}{m_{i,e}} \quad (3.10)$$

Since the plasma is isotropic, it is possible to define the applied field as

$$\mathbf{B}_0 = \hat{\mathbf{z}}B_0 \quad (3.11)$$

Defining θ as the angle between \mathbf{B}_0 and \mathbf{n} and assume \mathbf{n} is in the xz plane. Now n_{\parallel} and n_{\perp} can be defined as

$$n_{\parallel} = n \cos \theta \quad (3.12)$$

$$n_{\perp} = n \sin \theta \quad (3.13)$$

Therefore equation 3.1 can be written in matrix form as

$$\begin{pmatrix} S - n_{\parallel}^2 & -iD & n_{\parallel}n_{\perp} \\ iD & S - n_{\parallel}^2 + n_{\perp}^2 & 0 \\ n_{\parallel}n_{\perp} & 0 & P - n_{\perp}^2 \end{pmatrix} \begin{pmatrix} E_x \\ E_y \\ E_z \end{pmatrix} = 0 \quad (3.14)$$

If n_{\parallel} is set by the plasma parameters then it is possible to solve equation 3.14 for a non-trivial solution for n_{\perp} by setting the determinant of the matrix to zero. The solution is

$$An_{\perp}^4 + Bn_{\perp}^2 + C = 0 \quad (3.15)$$

where

$$A = S \quad (3.16)$$

$$B = (n_{\parallel}^2 - S)(S + P) + D^2 \quad (3.17)$$

$$C = P[(n_{\parallel}^2 - S)^2 - D^2] \quad (3.18)$$

Equation 3.15 has the general quadratic solution

$$n_{\perp}^2 = \frac{-B \pm \sqrt{B^2 - 4AC}}{2A} \quad (3.19)$$

When $B^2 \gg 4AC$ there are two real, distinct solutions to equation 3.19. These correspond to the fast and slow waves, $n_{\perp s}$ and $n_{\perp f}$ respectively. A plot of fast and slow wave roots are shown in Figure 3.1.

$$n_{\perp s}^2 = \frac{-P}{S}(n_{\parallel}^2 - S) - \frac{D}{S} \quad (3.20)$$

$$n_{\perp f}^2 = \frac{D^2 - (n_{\parallel}^2 - S)^2}{(n_{\parallel}^2 - S) + D^2/P} \quad (3.21)$$

At low values of n_{\parallel} , $B^2 = 4AC$, giving a single solution to equation 3.15 and the slow and fast wave are said to coalesce [71].

The helicon wave is a fast wave with a high index of refraction (i.e. $n_{\parallel}^2 \gg S, \frac{D^2}{P}$) and has a frequency greater than the ion cyclotron frequency and much less than the electron cyclotron frequency ($\omega_{ci} \ll \omega \ll \omega_{ce}$). Thus, equation 3.21 can be rewritten to give the helicon wave dispersion relation.

$$n_{\parallel}^2 n_{\perp f}^2 + n_{\parallel}^4 = D^2 \approx \left(\frac{\omega_{pe}^2}{\omega \omega_{ce}} \right)^2 \quad (3.22)$$

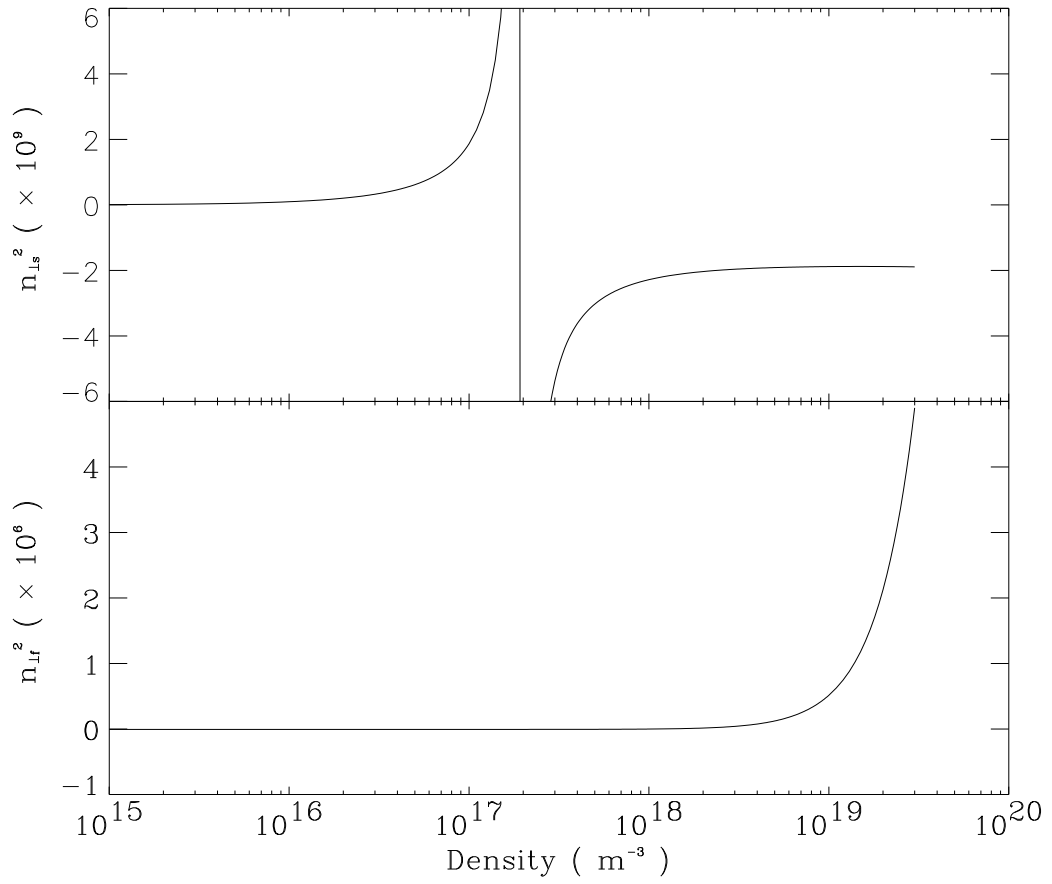


Figure 3.1: *The fast and slow wave roots for $n_{\parallel} = 75m^{-1}$, $B_0=768$ Gauss.*

Which can be re-written in terms of the wave number as

$$k_{\parallel}^2 k_{\perp}^2 + k_{\parallel}^4 = \left(\frac{\omega \omega_{pe}^2}{\omega_{ce} c^2} \right)^2 \quad (3.23)$$

3.2 Wavefields

The helicon wave dispersion relation, as well as the wavefield, can also be determined using Maxwell's equations and Ohm's law. Since the frequency range of the helicon wave is restricted to less than the electron cyclotron frequency and greater than the ion cyclotron frequency, electron inertia and ion motion may be neglected, simplifying Ohm's law. Maxwell's equations are

$$\nabla \times \mathbf{E} = \frac{-1}{c} \frac{\partial \mathbf{B}}{\partial t} \quad (3.24)$$

$$\nabla \times \mathbf{B} = \frac{4\pi}{c} \mathbf{j} \quad (3.25)$$

and the simplified Ohm's law is

$$\mathbf{E} = \frac{\mathbf{j} \times \mathbf{B}_0}{en_0} \quad (3.26)$$

where \mathbf{B}_0 is the applied static magnetic field which is defined to be in the $\hat{\mathbf{z}}$ direction (i.e. $\mathbf{B}_0 = B_0 \hat{\mathbf{z}}$), \mathbf{B} and \mathbf{E} are the magnetic and electric wavefields, \mathbf{j} is the current density, and n_0 is the plasma density. \mathbf{B} , \mathbf{E} and \mathbf{j} are assumed to vary as $e^{i(m\theta + k_{\parallel}z - \omega t)}$, where m is the azimuthal mode number and k_{\parallel} is the parallel wave number. Substituting equations

3.24 and 3.26 into equation 3.25 gives

$$\nabla \times \mathbf{B} = \alpha \mathbf{B} \quad (3.27)$$

where

$$\alpha = \frac{\omega \omega_{pe}^2}{k_{||} \omega_{ce} c^2} \quad (3.28)$$

$$\omega_{pe} = \sqrt{\frac{e^2 n_0}{\epsilon_0 m_e}} \quad (3.29)$$

The curl of equation 3.27 gives

$$\nabla^2 \mathbf{B} + \alpha^2 \mathbf{B} = \mathbf{0} \quad (3.30)$$

The $\hat{\mathbf{z}}$ component of equation 3.30 in cylindrical coordinates is

$$\frac{\partial^2 B_z}{\partial r^2} + \frac{1}{r} \frac{\partial B_z}{\partial r} + (k_{\perp}^2 - \frac{m^2}{r}) B_z = 0 \quad (3.31)$$

where k_{\perp} is the perpendicular wave number and k_{\perp} and $k_{||}$ are related through α by

$$\alpha^2 = k_{\perp}^2 + k_{||}^2 \quad (3.32)$$

Equations 3.32 and 3.28 combine to give the helicon wave dispersion relation as previously derived in equation 3.23. By substituting for the electron plasma frequency, equation 3.23 can be rearranged to relate the density and applied field to the parallel and

perpendicular wave numbers.

$$\frac{n_0}{B_0} = \frac{c}{4\pi e\omega} \left(k_{\parallel}^2 k_{\perp}^2 + k_{\parallel}^4 \right)^{\frac{1}{2}} \quad (3.33)$$

The components of the magnetic wavefields are obtained by solving equation 3.31 for B_z and substituting this back into equation 3.27 to obtain B_r and B_{θ} .

$$B_z = Ak_{\perp} J_m(k_{\perp} r) \quad (3.34)$$

$$B_r = \frac{iA}{k_{\perp}} \left(\frac{m\alpha}{r} J_m(k_{\perp} r) + k_{\parallel} J'_m(k_{\perp} r) \right) \quad (3.35)$$

$$B_{\theta} = -\frac{A}{k_{\perp}} \left(\frac{mk_{\parallel}}{r} J_m(k_{\perp} r) + \alpha J'_m(k_{\perp} r) \right) \quad (3.36)$$

where A is an arbitrary amplitude and J'_m is the partial differential of the Bessel function with respect to r . Examples of radial magnetic wavefields calculated using equations 3.34, 3.35, and 3.36 are shown in figure 3.2 for the first radial mode. It has been shown by Light and Chen [82] that the profiles for the $m = +1$ and $m = -1$ modes are similar when calculated using a conducting boundary condition.

The dispersion relation for a conducting wall boundary is easily found by setting $B_r = 0$ at the boundary. If the wall radius is a , then from equation 3.35

$$m\alpha J_m(k_{\perp} a) + k_{\parallel} a J'_m(k_{\perp} a) = 0 \quad (3.37)$$

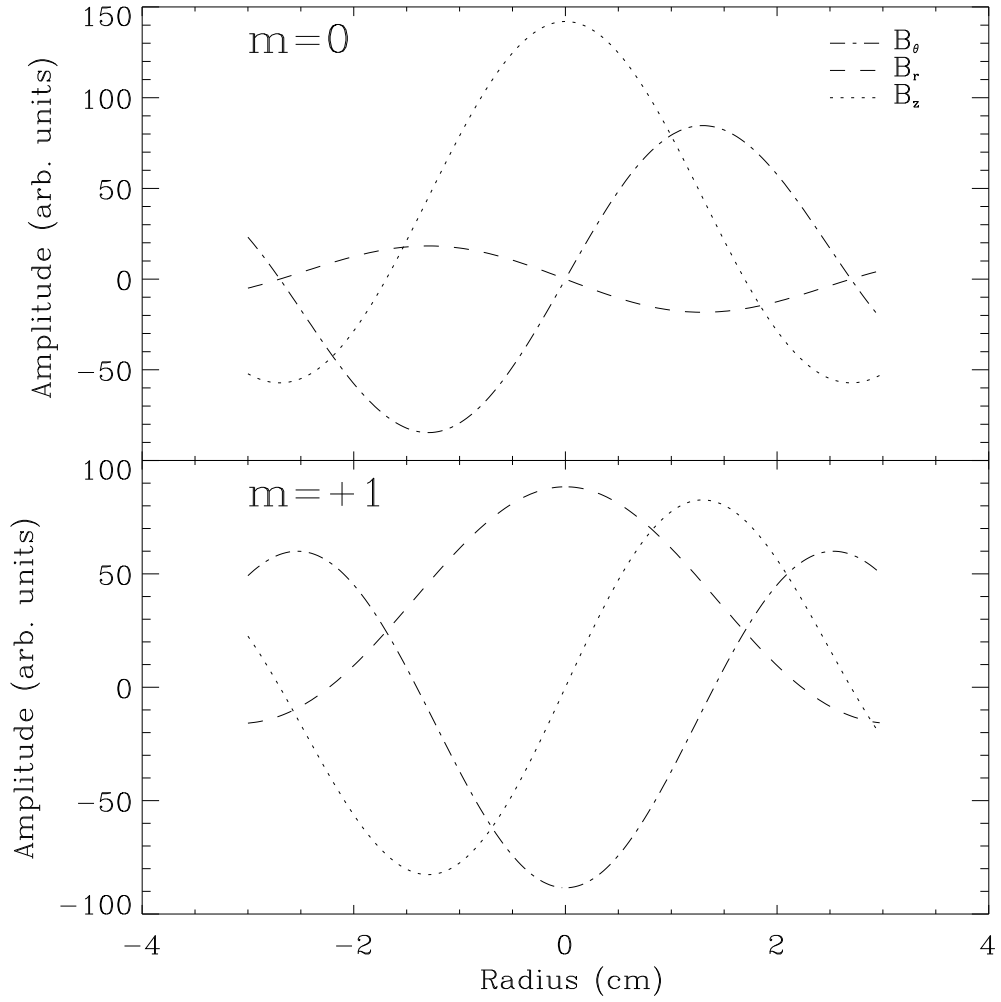


Figure 3.2: Plot of the wavefields for a conducting wall boundary of radius 2.25cm, $f=7\text{MHz}$, $k_{\parallel} = 31.5\text{m}^{-1}$, $B_0=768$ gauss.

From equation 3.37 the dependence of k_{\perp} on k_{\parallel} can be found, and their values can be substituted into equation 3.33 to give the dispersion relation.

Solutions for an insulating boundary are not as easily found as the condition enforced on B_r is now that it be continuous across the plasma boundary. The usual method of dealing with this is to numerically solve equation 3.33 to satisfy the boundary conditions. However, the experimental results presented in section 4.6 show that the assumption of an infinite plane wave, with $k_{\perp} \rightarrow 0$, holds for Basil conditions. This gives the simplified dispersion relation

$$k_{\parallel} \approx \sqrt{\frac{n_e \omega \mu_0 e}{B_0}} \quad (3.38)$$

It should be stressed that the theory presented in this section is for a uniform plasma. Also that the electron inertia is neglected, due to the frequency restriction stated earlier, which eliminates the possibility of the slow wave propagating.

3.3 Magnetohydrodynamic (MHD) Numerical Model

The results from the Basil experiment are compared to the results of a magnetohydrodynamic (MHD) numerical model by Kamenski [68]. This model uses the finite element method to solve Maxwell's equations for a cold cylindrical plasma inside a perfectly conducting cylinder with a vacuum gap between the the outer conducting boundary and the plasma. The outer conducting boundary corresponds to the inside of the magnetic field coils in the experimental setup. Unlike the experiment the antenna can be placed anywhere inside this cylinder, including in the plasma.

The model has features which include non-uniform radial electron density and tem-

perature profiles, which can be set to the measured plasma conditions. It is not necessary to consider boundary conditions at the antenna or plasma-vacuum interface as the model integrates smoothly over this region. Almost any antenna configuration can be employed and so far Kamenski has investigated double half-turn, $m = 0$ loop, double saddle coil, and helical antennas.

The model uses the 2×2 dielectric tensor of a cold collisional plasma, implying $\varepsilon_{33} = 0$

$$\varepsilon = \begin{pmatrix} \varepsilon_1 & i\varepsilon_2 \\ -i\varepsilon_2 & \varepsilon_1 \end{pmatrix} \quad (3.39)$$

This gives the wave equation

$$-\left[\alpha(rE_\theta)\right]' + \beta(rE_\theta) = -\left[\frac{\bar{\varepsilon}_2}{k_1^2}J_r + iJ_\theta + m\left(\frac{J_r}{k_1^2 r}\right)'\right] \quad (3.40)$$

The ' implies differentiation over the radial direction, $\frac{\partial}{\partial r}$.

$$\begin{aligned} \bar{\varepsilon}_{1,2} &= k_0^2 \varepsilon_{1,2} \\ J_{r,\theta} &= \frac{4\pi k_0}{c} j_{r,\theta} \\ k_0^2 &= \frac{\omega}{c} \\ \alpha(r) &= \frac{A}{k_1^2 r} \\ \beta(r) &= \frac{k_1^2}{r} + m\left(\frac{\bar{\varepsilon}_2}{k_1^2 r^2}\right)' \\ k_1^2 &= \frac{m^2}{r^2} - A \end{aligned}$$

$$\begin{aligned}
k_{\perp}^2 &= A + \frac{\bar{\varepsilon}_2}{k_{\perp}^2} \\
A &= \bar{\varepsilon}_1 - k_z^2 \\
\varepsilon_1 &= 1 - \sum_i \frac{\omega_{pi}^2(\omega + i\nu_i)}{\omega[(\omega + i\nu_i)^2 - \omega_{ci}^2]} - \frac{\omega_{pe}^2(\omega + i\nu_e)}{\omega[(\omega + i\nu_e)^2 - \omega_{ce}^2]} \\
\varepsilon_2 &= - \sum_i q \frac{\omega_{pi}^2 \omega_{ci}}{\omega[(\omega + i\nu_i)^2 - \omega_{ci}^2]} + \frac{\omega_{pe}^2 \omega_{ce}}{\omega[(\omega + i\nu_e)^2 - \omega_{ce}^2]}
\end{aligned}$$

Collisions (ion-electron, electron-electron, and ion-neutral) are included in the terms $\nu_i = \nu_{ie}$ and $\nu_e = \nu_{ee} + \sum_i \nu_{ei}$.

By comparison with the analytic solution for the uniform plasma dispersion relation the model was shown to describe the fast wave down to below the ion cyclotron frequency. High order radial modes are limited near their cutoffs by the omission of the electron mass, limiting perpendicular wave number. It is reported in this thesis that there is an experimentally observed effect near the lower hybrid resonance. The model does not explicitly include the lower hybrid wave, however, it is unlikely that the lower hybrid wave has been excited directly so the results of the model should not be adversely effected by any subsequent mode conversion.

The model calculates the wavefields, and from these the antenna impedance is calculated using the ‘‘induced emf’’ method. This is the first time radiation resistance has been accurately calculated and compared to experimental results for antennas used in helicon wave plasma production.

For specified density and temperature radial profiles, and antenna current, the code calculates theoretical radial and axial wavefields, which can be compared with the measured wavefields. The code also calculates the Poynting flux across the boundary at the

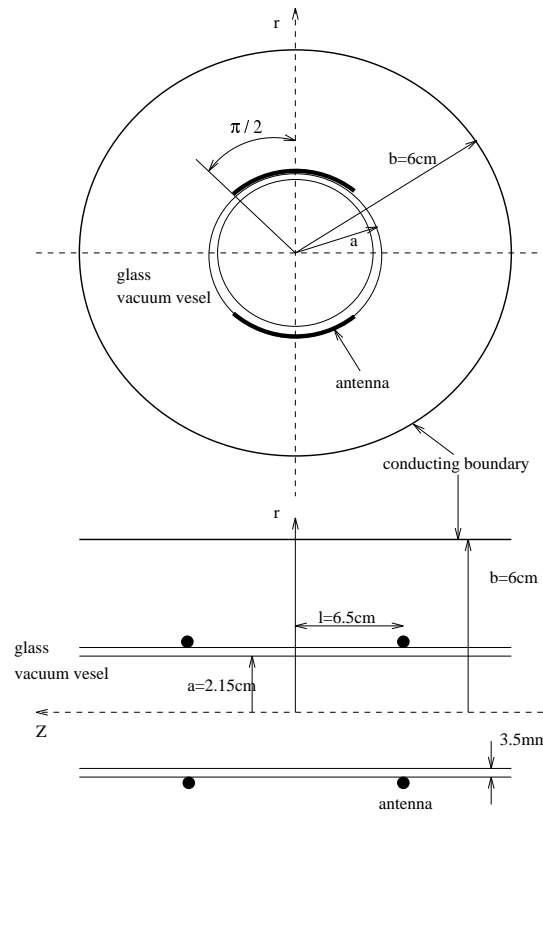


Figure 3.3: *The parameters used by the finite element method code for Basil with a double saddle coil antenna.*

edge of the plasma and the radiation resistance. Together with the antenna current can be used to calculate the plasma loading which can be compared to the measured loading.

3.4 Damping

In a perfectly collisionless plasma perturbation of the magnetic field perpendicular to B_0 would result in an electric field parallel to B_0 , E_z . This field would be cancelled by the space charge of the wave, which in the case of the helicon wave is due to the oscillating electrons. In the collisionless case the average energy transferred to the electrons is zero. However if the electrons undergo collisions an effective drag on the electron motion along B_0 is produced, which will result in a net E_z and the transfer of energy from the wave to the electrons, resulting in a damping of the wave. In the following analysis the static field is assumed to be large enough that perpendicular electron inertia and the finite Larmor radius of the electrons can be ignored, which is a valid assumption for the high fields in Basil.

3.4.1 Collisional Damping

By adding a collisional term to Ohm's law it is possible to derive a collisional damping length for the generalised collision frequency. This has been presented in a clear fashion by Chen [34]. Ohm's law can be written as

$$\mathbf{E} = \frac{\mathbf{j} \times \mathbf{B}_0}{en_0} - \frac{i\mathbf{m}_e}{n_0 e^2}(\omega + i\nu)\mathbf{j} \quad (3.41)$$

Following the approach in sections 3.2 equation 3.24, 3.25, and 3.41 can be combined to give

$$(\omega + i\nu)\nabla \times \nabla \times \mathbf{B} - k\omega_{ce}\nabla \times \mathbf{B} + \alpha k\omega_{ce}\mathbf{B} = \mathbf{0} \quad (3.42)$$

where α is defined in equation 3.28.

By factorising equation 3.42 and solving for the quadratic, the general solution can be found

$$\nabla \times \mathbf{B}_{1,2} = \beta_{1,2}\mathbf{B}_{1,2} \quad (3.43)$$

where,

$$\mathbf{B} = \mathbf{B}_1 + \mathbf{B}_2 \quad (3.44)$$

$$\beta_{1,2} = \frac{[1 \mp (1 - 4\alpha\gamma)^{1/2}]}{2\gamma} \quad (3.45)$$

$$\gamma \equiv \frac{(\omega + i\nu)}{k\omega_{ce}} \quad (3.46)$$

The root corresponding to the helicon wave is β_1 , which can be written in the form of equation 3.28, with the approximation of small $\alpha\nu$, as

$$\beta_1 = \alpha \left[1 + \left(\frac{\alpha c}{\omega_{pe}} \right)^2 \left(1 + \frac{i\nu}{\omega} \right) \right] \quad (3.47)$$

As in Section 3.2,

$$k_{\perp}^2 = \beta_1^2 - k_{\parallel}^2 \quad (3.48)$$

Thus, for a complex β_1 , k_{\parallel} must also be complex for the boundary conditions to be

satisfied.

$$k_{\parallel} = k_r + k_i \quad (3.49)$$

Defining the ratio, δ , between the imaginary and real components of k_{\parallel} as

$$\delta \equiv \frac{k_i}{k_r} \quad (3.50)$$

α can then be rewritten as,

$$\alpha = \frac{\alpha_0}{(1 + i\delta)} \quad (3.51)$$

where

$$\alpha_0 \equiv \frac{\omega \omega_{pe}^2}{k_r \omega_{ce} c^2} \quad (3.52)$$

Substituting equations 3.47, 3.48 into 3.51, and assuming δ and ν/ω are small, expanding to first order gives

$$\frac{k_i}{k_r} = \frac{\nu}{\omega} \left(\frac{\alpha_0 c}{\omega_{pe}} \right)^2 \left(1 + \frac{k_r^2}{\alpha_0^2} \right)^{-1} \quad (3.53)$$

The collisional damping length can then be found from

$$\lambda_c \approx \frac{1}{\text{Im}(k_{\parallel})} \quad (3.54)$$

For $k_{\perp} \ll k_{\parallel}$ this can be simplified to

$$\lambda_c \approx \frac{\omega}{\nu k_{\parallel}} \quad (3.55)$$

Density (m^{-3})	$kT_e(eV)$		
	3	4	5
0.5×10^{19}	$1.1 \times 10^8 S^{-1}$	$0.8 \times 10^8 S^{-1}$	$0.6 \times 10^8 S^{-1}$
1.0×10^{19}	$2.1 \times 10^8 S^{-1}$	$1.5 \times 10^8 S^{-1}$	$1.1 \times 10^8 S^{-1}$
5.0×10^{19}	$9.0 \times 10^8 S^{-1}$	$6.5 \times 10^8 S^{-1}$	$5.1 \times 10^8 S^{-1}$

Table 3.1: *Electron argon ion collision frequency as a function of electron temperature and density.*

If ν is taken to be the electron ion collision frequency, ν_{ei} , then in terms of the plasma resistivity, η

$$\eta = \frac{m\omega_{ei}}{n_0 e^2} \quad (3.56)$$

The collisional damping length is

$$\lambda_c \approx \frac{\omega\mu_0}{k_{||}^2 \eta} \quad (3.57)$$

Table 3.1 gives the argon electron ion collision frequency as a function of electron temperature and density while Figure 3.4 shows the argon electron neutral collision frequency as a function of filling pressure and electron temperature.

3.4.2 Landau Damping

Landau damping was first proposed as a damping mechanism for helicon waves by Dolgoplov et al [46], who called it Cherenkov absorption. Boswell [13] also suggested that Landau damping could be an explanation for the high damping rates measured, while Chen [34] suggested the high ionisation efficiency of helicon waves could be explained by Landau damping selectively exciting ionising electrons.

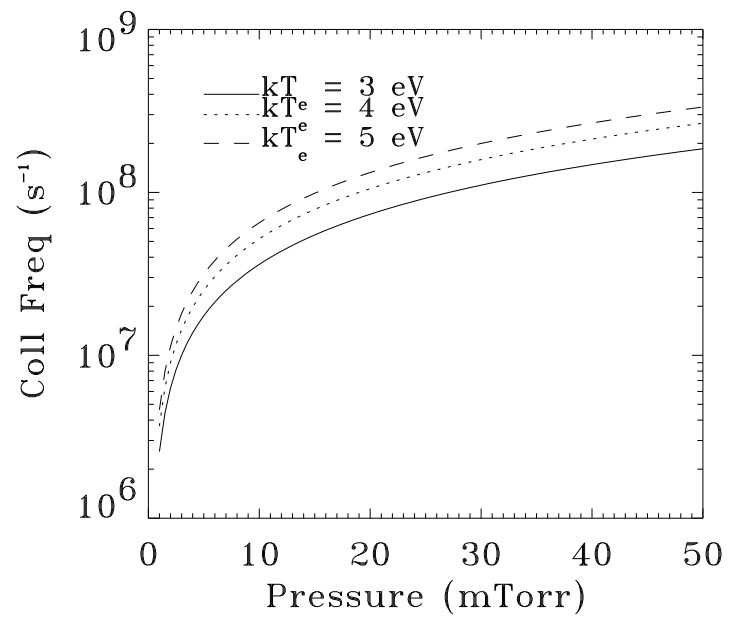


Figure 3.4: *Electron neutral collision frequency for Argon as a function of filling pressure and electron temperature.*

Chen [34] presents a derivation of Landau damping using simplifications applicable to Basil. Solving for j_z for the Boltzmann-Vlasov equations he finds an effective collision rate due to Landau damping

$$\nu_{LD} = 2\sqrt{\pi}\omega\xi^3 e^{-\xi^2} \quad (3.58)$$

where

$$\xi = \frac{\omega}{k_{\parallel}v_{th}} \quad (3.59)$$

The thermal velocity of the electrons, v_{th} being given by

$$v_{th} = \sqrt{\frac{2kT_e}{m_e}} \quad (3.60)$$

From equation 3.55 this gives a Landau damping length of

$$\lambda_{LD} = \omega_{ce} \left(2\sqrt{\pi}\omega k_{\parallel} \xi^3 e^{-\xi^2} \right)^{-1} \quad (3.61)$$

Landau damping becomes significant when the phase velocity of the wave is close to the thermal velocity of the electrons.